

The North Atlantic Oscillation and greenhouse-gas forcing

Svetlana I. Kuzmina,¹ Lennart Bengtsson,^{2,3,4} Ola M. Johannessen,^{5,6} Helge Drange,^{5,6,7} Leonid P. Bobylev,^{1,4} and Martin W. Miles^{8,9}

Received 21 July 2004; revised 19 November 2004; accepted 12 January 2005; published 17 February 2005.

[1] The results of 12 coupled climate models participating in the Coupled Model Intercomparison Project (CMIP2) are compared together with observational data in order to investigate: 1) How the current generation of climate models reproduce the major features of the winter North Atlantic Oscillation (NAO), and 2) How the NAO intensity and variability may change in response to increasing atmospheric CO₂ concentration. Long-term changes in the intensity and spatial position of the NAO nodes (Icelandic Low and Azores High) are investigated, and different definitions of the NAO index and the Arctic Oscillation (AO) are considered. The observed temporal trend in the NAO in recent decades lies beyond the natural variability found in the model control runs. For the majority of the models, there is a significant increase in the NAO trend in the forced runs relative to the control runs, suggesting that the NAO may intensify with further increases in greenhouse-gas concentrations. **Citation:** Kuzmina, S. I., L. Bengtsson, O. M. Johannessen, H. Drange, L. P. Bobylev, and M. W. Miles (2005), The North Atlantic Oscillation and greenhouse-gas forcing, *Geophys. Res. Lett.*, 32, L04703, doi:10.1029/2004GL021064.

1. Introduction

[2] The North Atlantic Oscillation (NAO) is a major mode of atmospheric variability in the Northern Hemisphere. The NAO is a measure of the atmospheric pressure difference between the Icelandic Low (IL) and Azores High (AH) centers of action – stronger than average gives a positive index value (NAO+) and v.v. The NAO is particularly important in winter, exerting a strong control on the Northern Hemisphere extra-tropical climate, e.g., modulating the westerly jet stream and temperature from eastern North America into Eurasia [Walker and Bliss, 1932; Wallace and Gultzer, 1981; Lamb and Pepler, 1987; Hurrell, 1995, 1996]. The NAO can be considered the dominant regional feature of the broader Arctic Oscillation

(AO) [Thompson and Wallace, 1998] or Northern Annular Mode (NAM) [Thompson and Wallace, 2001] of atmospheric pressure in the Northern Hemisphere, rather than a dynamically separate phenomenon – at least in winter, when they are arguably inseparable [Deser, 2000; Wallace, 2000].

[3] The NAO has exhibited a positive trend since the 1960s and it has been speculated that this may be linked to global warming, e.g., induced by anthropogenic increases in atmospheric greenhouse gases (GHGs). However, distinguishing natural versus anthropogenic variability in the NAO based on observed sea level pressure (SLP) alone is challenging. There are also uncertainties in the theoretical response of NAO/AO to enhanced greenhouse warming and our ability to model it realistically using numerical climate models [Delworth and Knutson, 2000; Shindell et al., 2001; Frauenfeld and Davis, 2003; Gillett et al., 2003]. The goal of the paper is to assess how well the current generation of climate models reproduces the general features of the observed winter NAO and to quantify changes in NAO under external forcing. Achievement of this goal requires 1) an assessment of the individual models, 2) an assessment of the ensemble mean of the models, and 3) an investigation of the future climate projections. Here, to investigate the NAO change as a response to increasing GHG forcing, the results of 12 coupled atmosphere–ocean numerical models participating in the Coupled Model Intercomparison Project (CMIP2) are used together with observational data.

2. Data and Methods

[4] We employ monthly-mean SLP fields for the entire Northern Hemisphere from 12 CMIP2 models as specified in Table 1. For documentation and validation of these models see the CMIP Web site at <http://www-pcmdi.llnl.gov/cmip/>. We have chosen the models with full-length runs without missing values and include only one model from each modeling center (e.g., only HADCM3, not HadCM2, from the Hadley Centre). For each model, two 80-y experiments are used: 1) a “control” simulation, representing natural variability (CMIP control runs use different constant atmospheric CO₂ concentrations, ranging from 290 to 353 ppm) and 2) a “forced” run perturbed by a 1% per year increase in atmospheric CO₂ concentration starting from the present-day climate state, where CO₂ doubles at about year 80 [Covey, 1998]. The CMIP2 idealized scenario with 1% per year CO₂ increase is only used for model sensitivity tests and is not meant to be representative for present or earlier emissions. However, the radiation forcing corresponding to the CMIP2-protocol cannot be ruled out in the future. In addition, the observed variations in NAO could be caused by natural variations in the climate system. It is presently hard to uniquely state which of the two

¹Nansen International Environmental and Remote Sensing Center, St. Petersburg, Russia.

²Max Planck Institute for Meteorology, Hamburg, Germany.

³Also at Environmental Systems Science Centre, University of Reading, Reading, UK.

⁴Also at Nansen Environmental and Remote Sensing Center, Bergen, Norway.

⁵Nansen Environmental and Remote Sensing Center, Bergen, Norway.

⁶Also at Geophysical Institute, University of Bergen, Bergen, Norway.

⁷Also at Bjerknes Centre for Climate Research, Bergen, Norway.

⁸Bjerknes Centre for Climate Research, Bergen, Norway.

⁹Also at Environmental Systems Analysis Research Center, Boulder, Colorado, USA.

Table 1. Statistical Significance (s) of the Difference Between Linear Trends in the NAO in the Control and Forced Runs for 12 CMIP2 Models^a

Index	NAO					MODEL *						
	BCM	BMR	CCC	CCSR	CERF	CSIR	ECHAM	GFDL	IAP	MRI	PCM	UKMO3
NAO1	<0.01	0.18	0.13	0.04	0.38	0.25	<0.01	0.56	0.03	0.25	<0.01	0.43
NAO2	0.04	0.01	<0.01	0.73	0.16	0.29	0.01	0.13	0.43	<0.01	0.02	0.65
NAO2	0.04	0.01	<0.01	0.73	0.16	0.29	0.01	0.13	0.43	<0.01	0.02	0.65
NAO3	0.08	0.28	0.01	0.32	0.43	0.64	0.18	0.49	0.05	0.19	0.37	0.32
NAO4	<0.01	0.05	<0.01	0.15	0.58	0.92	<0.01	0.65	0.02	0.22	<0.01	0.17
AO	0.06	0.63	<0.01	0.20	0.13	0.52	0.03	0.23	<0.01	0.29	<0.36	0.24

^aThe trends significant above the 95% confidence level ($s < 0.05$) are highlighted in bold. The NAO indices are defined in the text and model codes are defined as follows. Model Codes and Countries: BCM-Bergen Climate Model (Norway); BMR-Bureau of Meteorology Research Center (Australia); CCC-Canadian Center for Climate Modelling and Analysis (Canada); CCSR-Center for Climate System Research (Japan); CERF-Centre European de Recherch et de Formation Avancee en Calcul Scientifique (France); CSIR-Commonwealth Scientific and Industrial Research Organization (Australia); ECHAM - DKRZ/MPI (Germany); GFDL-Geophysical Fluid Dynamics Laboratory (USA); IAP-LASG / Institute for Atmospheric Physics (China); MRI-Meteorological Research Institute (Japan); PCM-DOE Parallel Climate Model (USA); UKMO3-United Kingdom Met. Office HadCM3 model (UK).

alternatives are most likely. The model data are available on a variety of grids; to facilitate intercomparison, all the model data are interpolated to a $2.5^\circ \times 2.5^\circ$ regular grid.

[5] Monthly-mean gridded dataset based on observations is also used: NCEP/NCAR re-analysis data from 1948 [Kalnay *et al.*, 1996, with updates]. In addition we use time series of station SLP comprising the Jones *et al.* [1997] NAO index. These are Gibraltar (36°N , 5.5°W) and a southwest Iceland time series, based mainly on Reykjavik (64.1°N , 22°W) both extending from 1823 to 2000. The locations are indicated in Figure 1a.

[6] Winter is defined here as November–April (NDJFMA). For the model integrations, SLP anomaly fields were obtained on the basis of the control run’s long-term winter mean. The spatial SLP distribution was investigated by applying Principal Component Analysis (PCA) for both the North Atlantic region (20°N – 80°N , 100°W – 20°E) and for the area north of 20°N . The latitude–longitude position of the IL center (φ_N , λ_N) was first approximated as the location of the minimum P_{\min} of the pressure field $P_{i,j}$ on the latitude–longitude grid (φ_i , λ_j) of the pressure field for latitudes poleward of 55°N . Its exact position was then found as the center of gravity of the pressure field using weighted anomalies. For instance, $\varphi_N = \sum \varphi_i P_{i,j} / \sum P_{i,j}$, where summation is spread over grid nodes where $P_{i,j} < P_{\min} + \Delta P$, and ΔP is estimated as 5hPa. The AH center (φ_S , λ_S) is defined in a similar way for latitudes south of 45°N .

[7] Four different definitions of the NAO index are considered: 1) Absolute SLP difference between Gibraltar

and Iceland (NAO₁); 2) Absolute SLP difference between the centers of the IL and AH (NAO₂); 3) Difference of SLP averaged over a northern (80°W – 30°E , 55°N – 80°N) and southern (80°W – 30°E , 20°N – 55°N) Atlantic region (NAO₃); and 4) First principal component (PC1) time series corresponding to a pressure-field PC pattern (NAO₄) for the North Atlantic region (20°N – 80°N , 100°W – 20°E). Absolute SLP differences were used for the calculation of NAO index, because standardization could hide errors in the model simulations. For the model data, the NAO₁ index was defined through interpolation from the model grid cells nearest to Gibraltar and Iceland. We also calculated the AO index as PC1 for the area north of 20°N . For each of the four NAO definitions and the AO, temporal trends were then calculated for the observations and models. Clearly, pattern-based indexes provide more information about the main features of SLP distribution than a two-point pressure difference. The statistical significance of the difference between trends for the control and forced run was found for each model, considering maximum difference between trends standardized by the sum of their standard deviations. Confidence level of the difference between trends was found as an error function of normalized maximum difference between trends.

3. Results

[8] It is found that the models realistically reproduce the IL and AH; e.g., broadly similar patterns in mean winter SLP in both observations and the models (Figure 1a). We

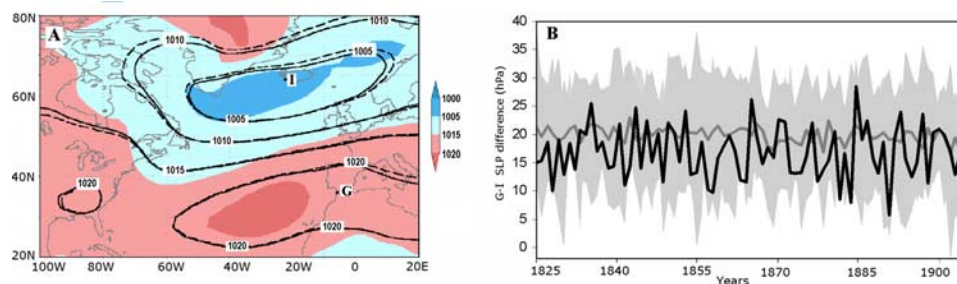


Figure 1. (a) Mean winter SLP (hPa) averaged across models (control runs – solid line, forced runs – dashed line) and NCEP/NCAR reanalysis data based on observations (color, shaded). The locations of the Gibraltar (G) and Iceland (I) stations of the Jones *et al.* [1997] NAO index are indicated. (b) Absolute SLP difference between G and I for observations (black line) and averaged across model control runs (gray line), as well as an envelope, containing 80-year individual control runs (gray shading).

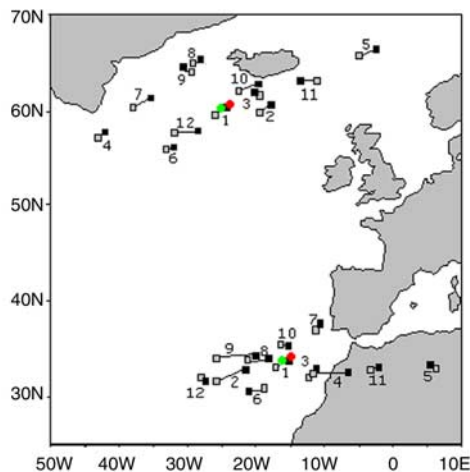


Figure 2. Mean locations of winter centers of IL and AH in 12 CMIP2 models (Table 1) and observations. Red – 12-model control mean, Green – Observed (NCEP/NCAR re-analysis data). Numbers indicate the individual models: 1 - BCM, 2 - BMR; 3 - CCC, 4 - CCSR, 5 - CERF, 6 - CSIR, 7 - ECHAM4/OPYC3, 8 - GFDL, 9 - IAP, 10 - MRI, 11 - PCM, 12 - UKMO3; Gray – Control run, Black - Forced run.

find that the NAO pressure patterns are captured as realistically as the NAO-like temperature pattern that *Stephenson and Pavan* [2003] used as an NAO surrogate in their CMIP1 model study. The 12-model control-run mean SLP difference between Gibraltar and Iceland (i.e., *Jones et al.* [1997] NAO index) lies close to observations, with an ensemble-mean difference from the observations ~ 3 hPa and the mean inter-model standard deviation ~ 7 hPa (Figure 1b). The model ensemble-mean locations of the pressure centers are nearly identical to the observations, though with some between-model scatter (Figure 2). The observations indicate that the IL and AH comprise a unified system varying synchronously – their centers simultaneously shift position along a southwest–northeast axis, with a northeastward shift occurring during maximum SLP gradient (i.e., strong NAO⁺). Most of the model runs also exhibit this tendency to shift position.

[9] Spatial and temporal differences between the control and forced runs are evident. Spatially, a northeastward shift (Figure 2) in the centers of the IL and AH is found in the forced run compared with the control run for most of the models. This shift is statistically significant at 95% confidence level for the models except CERF, CSIR, MRI and PCM. For most of the forced runs, low pressure at high latitudes spreads over a vaster area with even slight changes of SLP in the IL and AH centers of action.

[10] Temporally, the most interesting result is a difference between trends in the forced and control runs. Figure 3 shows modeled (control and forced) linear trends for the NAO indices (NAO_{1–4}) and the AO index, for each model as well as the ensemble mean of the models. The result shows that for the majority of the models and more or less independent of the index being used, there is a relative increase in the trend between the control and forced integrations [cf. *Schneider et al.*, 2003]. It is noted that the control integrations characteristically have small nega-

tive trends for each index, though these are not statistically significant at the 95% confidence level, except BMR, CCSR and PCM. This is an indication of model deficiency and possibly the limited length of the runs. Nevertheless, it should be recalled that the climate experiment in CMIP2 is essentially a “perturbation integration” and therefore the main interest is the *change* in the trend between the control and the forced experiment.

[11] The three pattern-based indices – NAO₃, NAO₄ and the AO – show more consistent model-to-model trends than NAO₁ and NAO₂ and are positive for all forced runs, except for CCSR (NAO₃ and AO), CSIR (NAO₄) and GFDL (NAO₄). Regarding statistical significance, the difference between linear trends in the control and forced runs is more meaningful than the significance of individual trends, as mentioned above. Table 1 indicates that control versus forced trend differences from 8 of the 12 models (BCM, BMR, CCC, CCSR, ECHAM, IAP, MRI and PCM) are statistically significant at $s < 0.05$ (i.e., >95% confidence level) for at least one index. Three models (CERF, GFDL and UKMO3) have $s < 0.20$, while $s > 0.20$ for the CSIR model.

[12] Further, we calculated successive 30-yr linear trends for NAO₁ from control and perturbed runs, as well as for the NAO₁ calculated from observational data (Figure 4). The observed NAO₁ trends in recent decades are outside the 95% confidence range of variability simulated during

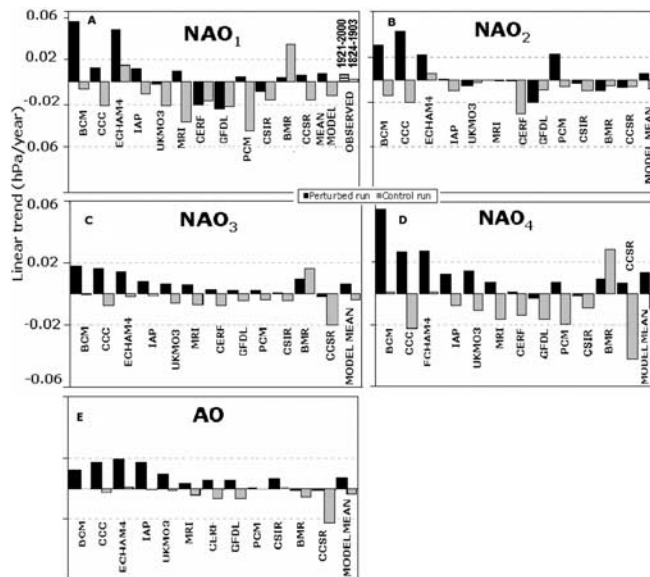


Figure 3. Linear trends (hPa/year) for the four NAO indexes calculated as (a) SLP difference between Gibraltar and Iceland (NAO1); (b) SLP difference between the centres of action (NAO2); (c) first SLP principal component (PC) for the Atlantic region (NAO3); (d) difference between averaged SLP for the north (80°W–30°E, 55°N–80°N) and south (80°W–30°E, 20°N–55°N) Atlantic sectors (NAO4), (e) AO index, PC1 for the area north of 20°N. Gray columns – Control run. Black columns – Forced run. For NAO1 (a): Gray dotted column (upper right) – observed, “control period” (1824–1903, essentially without anthropogenic contribution). Black stippled column (upper right) – Observed, “forced period” (1921–2000).

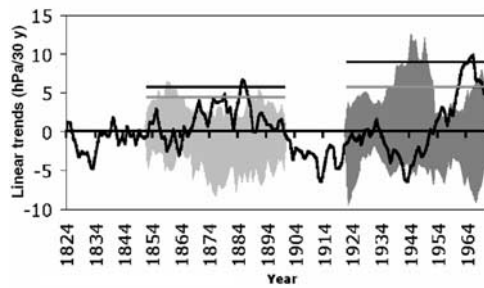


Figure 4. 30-yr linear NAO₁ trends (hPa/30 yr) for observations (black curve) and an envelope containing the individual control (light gray shading) and forced (dark gray shading) model simulations. Trends were computed with 1-yr increments. X-axis labels indicate the starting year of 30-yr trends; i.e., 1964 indicates 1964–1993. Solid horizontal lines show the mean 95% confidence levels computed across the models (gray line) and observations (black line).

control runs, and this could be interpreted partly as internal variability. The observed NAO₁ index has its largest positive trends during the period 1961–1999 (>6 hPa/30 yr) with a maximum (9.8 hPa/30 yr) from 1966–1996, in contrast to the control experiments, where no trends were larger than 6.6 hPa/30 yr. For the forced runs, maximum trends exceed the observations in three models (13 hPa/30 yr (CCSR), 9.4 hPa/30 yr (MRI), 8.2 hPa/30 yr (GFDL)), while six models range from 4–6 hPa/30 yr and three models exhibit trends of ~3 hPa/30 yr. These results suggest that some response to GHG forcing could be present in the observed NAO index record, indicating a possible increase of the NAO positive phase.

4. Conclusion

[13] We find that the current generation of climate models reproduces, on average, the main SLP features of the observed winter NAO. The recent trend observed in the NAO lies beyond the natural variability found in the control runs. Furthermore, the forced runs have greater NAO intensity than the control runs, indicating that the NAO may intensify with further increases in atmospheric GHG concentrations. The underlying causes of forced variability in the North Atlantic region are unclear. There are at least two candidate mechanisms to explain the recent trend of the NAO: An extra-tropical response to changes in tropical sea-surface temperature (SST) [Hoerling *et al.*, 2001; Lin *et al.*, 2002] and another involving stratospheric changes [Baldwin and Dunkerton, 2001]. In either case, the processes linking the NAO to GHG forcing need further elucidation.

[14] **Acknowledgment.** This work was supported by grants from the European Union's 5th Framework Programme project "Arctic Ice Cover

Simulation Experiment (AICSEX)," and the Research Council of Norway's Polar Climate Research project "Marine Climate and Ecosystems in the Seasonal Ice Zone (MACESIZ)."

References

- Baldwin, M. K., and T. J. Dunkerton (2001), Stratospheric harbingers of anomalous weather regimes, *Science*, 294, 581–584.
- Covey, C. (1998), CMIP1 model output, Program for Climate Model Diagnostics and Intercomparison (PCMDI), Lawrence Livermore Natl. Lab., Livermore, Calif. (Available at <http://www-pcmdi.lln.gov/cmip/diagsub.html>)
- Delworth, T. L., and T. R. Knutson (2000), Simulation of early 20th century global warming, *Science*, 287, 2246–2250.
- Deser, C. (2000), On the teleconnectivity of the "Arctic Oscillation", *Geophys. Res. Lett.*, 27, 779–782.
- Frauenfeld, O. W., and R. E. Davis (2003), Northern hemisphere circumpolar vortex trends and climate change implications, *J. Geophys. Res.*, 108(D14), 4423, doi:10.1029/2002JD002958.
- Gillet, N. P., et al. (2003), Climate change and the North Atlantic Oscillation, in *The North Atlantic Oscillation: Climate Significance and Environmental Impact*, *Geophys. Monogr. Ser.*, vol. 134, edited by J. W. Hurrell *et al.*, pp. 193–209, AGU, Washington, D.C.
- Hoerling, M. P., et al. (2001), Tropical origins for recent North Atlantic climate change, *Science*, 292, 90–92.
- Hurrell, J. W. (1995), Decadal trends in the North Atlantic Oscillation: Regional temperature and precipitation, *Science*, 269, 676–679.
- Hurrell, J. W. (1996), Influence of variations in extratropical wintertime teleconnections on Northern Hemisphere temperatures, *Geophys. Res. Lett.*, 23, 665–668.
- Jones, P. D., et al. (1997), Extension to the North Atlantic Oscillation using early instrumental pressure observations from Gibraltar and South-West Iceland, *Int. J. Climatol.*, 17, 1433–1450 (Available at <http://www.cru.uea.ac.uk/cru/data/nao.htm>)
- Kalnay, E., et al. (1996), NCEP/NCAR 40-year reanalysis project, *Bull. Am. Meteorol. Soc.*, 77, 437–471.
- Lamb, P. J., and R. A. Pepler (1987), North Atlantic Oscillation: Concept and an application, *Bull. Am. Meteorol. Soc.*, 68, 1218–1225.
- Lin, H., et al. (2002), Tropical links of the Arctic Oscillation, *Geophys. Res. Lett.*, 29(20), 1943, doi:10.1029/2002GL015822.
- Schneider, E. K., et al. (2003), Forcing of Northern Hemisphere climate trends, *J. Atmos. Sci.*, 60, 1504–1521.
- Shindell, D. T., et al. (2001), Northern Hemisphere winter climate response to greenhouse gas, ozone, solar, and volcanic forcing, *J. Geophys. Res.*, 106, 7193–7210.
- Stephenson, D. B., and V. Pavan (2003), The North Atlantic Oscillation in coupled climate models: A CMIP1 evaluation, *Clim. Dyn.*, 20, 381–399.
- Thompson, D. J. W., and J. M. Wallace (1998), The Arctic Oscillation signature in the wintertime geopotential height and temperature fields, *Geophys. Res. Lett.*, 25, 1297–1300.
- Thompson, D. W. J., and J. M. Wallace (2001), Regional climate impacts of the Northern Hemisphere Annular Mode, *Science*, 293, 85–89.
- Walker, G. T., and E. W. Bliss (1932), World weather, V, *Mem R. Meteorol. Soc.*, 4, 53–84.
- Wallace, J. M. (2000), North Atlantic Oscillation/annular mode, Two paradigms – one phenomenon, *Q. J. R. Meteorol. Soc.*, 126, 791–805.
- Wallace, J. M., and D. S. Gutzler (1981), Teleconnections in the geopotential height field during the Northern Hemisphere winter, *Mon. Weather Rev.*, 109, 784–812.
- L. Bengtsson, Max Planck Institute for Meteorology, Bundesstr. 55, D-20146 Hamburg, Germany.
- L. P. Bobylev and S. I. Kuzmina, Nansen International Environmental and Remote Sensing Center, Bolshaya Monetnaya str., 26/28, 197101 St. Petersburg, Russia. (svetlana.kuzmina@niersc.spb.ru)
- H. Drange and O. M. Johannessen, Nansen Environmental and Remote Sensing Center, Thormøhlensgate 47, N-5006 Bergen, Norway.
- M. W. Miles, Bjerknes Centre for Climate Research, Allegaten 70, N-5007 Bergen, Norway.